JOURNAL OF SOLID STATE CHEMISTRY **133,** 356–364 (1997)
ARTICLE NO. SC977582

High-Pressure, High-Temperature Syntheses in the B–C–N–O System

I. Preparation and Characterization

Hervé Hubert,*,[1] Laurence A. J. Garvie,† Peter R. Buseck,† William T. Petuskey,* and Paul F. McMillan*

*Materials Research Center, Department of Chemistry and Biochemistry, and †Departments of Geology and Chemistry & Biochemistry, Arizona State University, Tempe, Arizona 85287

Received August 4, 1997; accepted August 4, 1997

We synthesized several α-rhombohedral B-rich materials belonging to the B–C–N–O system using a multianvil press. B–C–O materials were prepared by reacting mixtures of B, C, and B_2O_3 in the 5 to 7.5 GPa pressure range and at a temperature of 1700°C. Powder X-ray diffraction and parallel electron energy-loss spectroscopy with a transmission electron microscope showed that the $B_xC_yO_z$ phases obtained are based on the α-rhombohedral B structure. Crystals of composition $B_6C_{1.1}O_{0.33}$ to $B_6C_{1.28}O_{0.31}$ ranging in size from 1 to 20 μm were grown. Small transparent lustrous red cleavage flakes were obtained for stoichiometries close to B_6O. The growth of boron carbide nanorods was also observed in some of the run products. We report the first conclusive bulk synthesis of a new boron nitride, B_6N_{1-x}, obtained by reacting B and hexagonal BN at 7.5 GPa and 1700°C. The structure of this compound is derived from that of α-rhombohedral B (space groupe $R\bar{3}m$) and the refined hexagonal cell parameters are $a_h = 5.457$ Å and $c_h = 12.241$ Å. © 1997 Academic Press

1. INTRODUCTION

Boron-rich solids give rise to a large family of refractory compounds, many with unique crystal structures, and a range of interesting physical and chemical properties related to their short interatomic bond lengths and their predominantly covalent character (1). The structure of boron suboxide, nominally B_6O, and the family of carbides "B_4C" are related to that of α-rhombohedral boron ($R\bar{3}m$ space group) as illustrated in Fig. 1. The α-rhombohedral B framework consists of 8 B_{12} icosahedral units located at the vertices of a rhombohedral cell (Fig. 1a). In B_6O, the O are located in the interstices along the [111] rhombohedral axis and trigonally bonded to three B in three separate icosahedra (Fig. 1b). Boron carbide compounds exist as a single phase over a wide range of compositions from $B_{10}C$ to near stoichiometric B_4C ($B_{4.3}C$). A structural model has been proposed for the "B_4C" solid solution by Emin (2). For a composition near B_4C, the framework consists of $B_{11}C$ icosahedra and CBC atom chains situated along the main diagonal of the rhombohedral cell (Fig. 1c). For lower carbon concentrations, CBC chains are substituted by CBB chains, leading to $B_{13}C_2$, ($B_{11}C$)(CBB), for a near complete substitution. For carbon concentrations lower than $B_{13}C_2$, some $B_{11}C$ icosahedra are replaced by B_{12} icosahedra.

Because of its mechanical properties, boron carbide is utilized as an armor component and as a grinding material, as well as a neutron absorber in nuclear reactors. It has potentially useful thermal and electronic properties, e.g., for thermoelectric power generation (2, 3). B_6O qualifies as a "superhard phase" having a microhardness of 38 GPa (4), greater than TiB_2 (34 GPa), TiC (32 GPa), W_2C (30 GPa), and B_4C (28 GPa) (5). Other interesting properties of this compound are its low density and chemical inertness. These characteristics make B_6O potentially useful as an abrasive and for high-wear applications. In addition to the end-member α-rhombohedral B-rich solids, such as B_4C and B_6O, it is interesting to investigate the structures and properties of intermediate materials in the B–C–O system that could display unique electronic and physical characteristics.

Here, we describe the high-pressure and high-temperature synthesis of new phases and a possible solid solution series in the B_6O–B_4C system. We also report the first conclusive bulk synthesis of a new boron nitride, B_6N_{1-x}.

2. EXPERIMENTAL

A Walker-type multianvil apparatus was used to carry out the high-pressure, high-temperature syntheses (6). The

[1]To whom correspondence should be addressed. E-mail: hubert@asu.edu.

0022-4596/97 $25.00

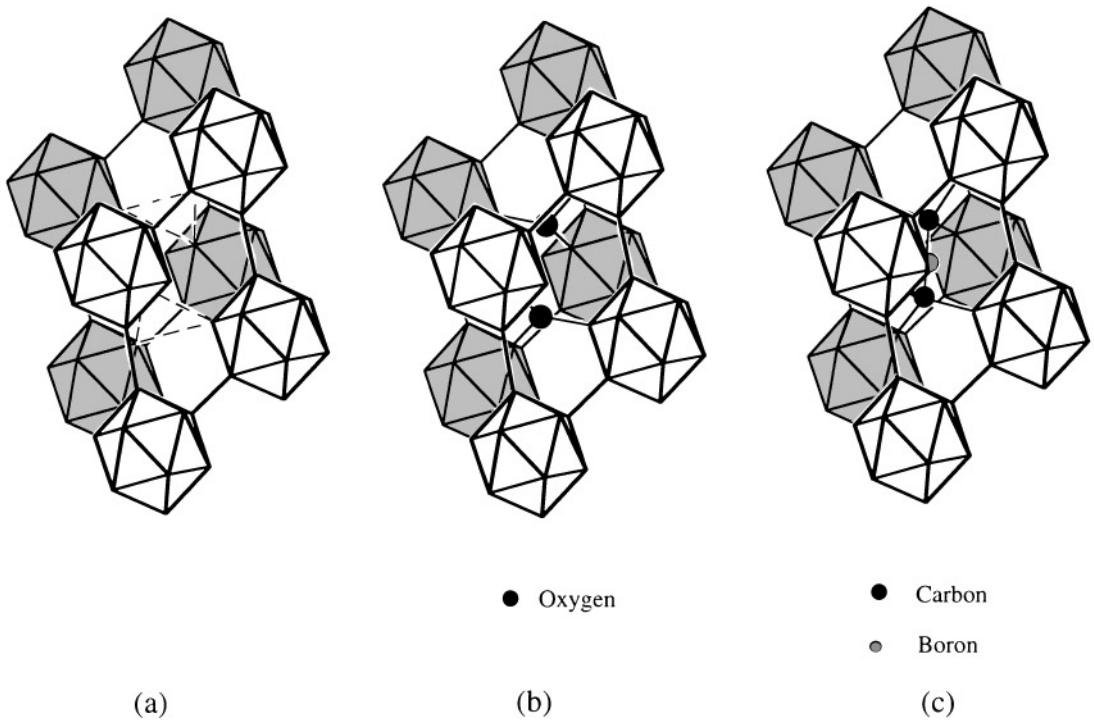

FIG. 1. Structure of α-rhombohedral boron (a) and two materials based on the α-rhombohedral B structure: (b) B_6O and (c) B_4C. The structure of α-rhombohedral boron consists of 8 B_{12} icosahedra at the apices of a rhombohedral unit cell. Shaded icosahedra are in the background.

pressure medium consisted of an MgO octahedron, and force was applied by eight WC cubes with corners truncated to triangular faces. The cell assembly is illustrated in Fig. 2.

The reduction of B_2O_3 by B leads to the formation of B_6O (4, 7, 8):

$$16\,B + B_2O_3 \rightarrow 3\,B_6O. \qquad [1]$$

TABLE 1
Summary of the Runs

Run	Initial mixture	*P* (GPa)	*T* (°C)	*t* (mn)	Products	
					XRD	PEELS
519	$16B + 2C + 3B_2O_3$	7.5	1700	30	$B_xC_yO_z$[a]	$B_6C_{0.66}O_{0.66}$-$B_6C_{0.45}O_{0.77}$
521	$16B + 4C + 3B_2O_3$	7.5	1700	30	$B_6C_xO_y$	$B_6C_{1.1}O_{0.33}$
524	$16B + 4C + 3B_2O_3$	5	1700	5	$B_6C_xO_y$	$B_6C_{1.28}O_{0.31}$
532	$16B + 4C + 3B_2O_3$	7.5	1700	30	$B_6C_xO_y$	$B_6C_{1.1}O_{0.33}$
545	$16B + 4C + B_2O_3$	7.5	1700	30	B_4C	B_4C
546	$16B + 2C + B_2O_3$	7.5	1700	30	$B_6O + B_4C$	$B_6C_{1.28}O_{0.2}$-$B_6C_{0.58}O_{0.46}$[b]
549	$16B + 2C + B_2O_3$	7.5	1700	300	$B_6O + B_4C$	$B_6C_{1.28}O_{0.2}$-$B_6C_{0.58}O_{0.46}$[b]
550	$16B + C + B_2O_3$	7.5	1700	30	$B_6O + B_4C$	$B_6C_{0.2}O_{0.83}$-$B_6C_{1.2}O_{0.24}$[b]
576	$5B + BN$	7.5	1700	30	B_6N_{1-x}[c]	$B_6N_{0.92}$[c]
586	$5B + BN$	7.5	1700	30	B_6N_{1-x}[c]	$B_6N_{0.92}$[c]
451	$16B + 2B_2O_3$	5.5	1800	5	B_6O	B_6O
555	$16B + B_2O_3$	7.5	1700	30	B_6O[d]	B_6O[d]

Note. The products (washed in water) were determined using XRD and PEELS.
[a]Several phases according to XRD data.
[b]Composition range acquired by PEELS.
[c]B_6N_{1-x} present in the majority of the sample along with hBN, cBN, β-rhombohedral B, and amorphous B.
[d]B_6O present in the majority of the sample along with amorphous B.

Preparation of $B_xC_yO_z$ phases were conducted in two sets of experiments in which amorphous B (99.999%), B_2O_3 (99.99%), and C (99.999%) were mixed in various ratios (Table 1). In the first series of runs, different concentrations of carbon were added to a mixture having a B/B_2O_3 molar ratio of 16/3:

$$16\,B + xC + 3\,B_2O_3, \quad x = 2, 4. \qquad [2]$$

The second set of experiments were performed with less B_2O_3, and the starting materials were mixed in the following proportions:

$$16\,B + xC + B_2O_3,\ x = 1, 2, 4. \qquad [3]$$

Attempts to prepare a nitride analogue of B_6O were also made. Amorphous B and hexagonal BN were mixed in ethanol according to the proposed reaction

$$5B + BN \rightarrow B_6N. \qquad [4]$$

The mixtures, prepared according to Eqs. [1]–[4], were pressed into pellets and enclosed in a hexagonal BN capsule. The encapsulated material was then placed in a graphite resistance furnace. Samples were pressurized to between 5 and 7.5 GPa and then heated at 1700°C for 30 min. Temperature inside the cell was calibrated with a W-5%Re/W-25%Re thermocouple.

The recovered materials were examined by optical microscopy, then gently ground between two WC cubes, and analyzed by powder X-ray diffraction (XRD) and parallel electron energy-loss spectroscopy (PEELS) before and after being washed in water to remove soluble materials. A Siemens D5000 powder X-ray diffractometer, employing Cu$K\alpha$ radiation, was used to identify the resulting phases. PEELS was used to characterize the different $B_xC_yO_z$ phases and determine their compositions. PEELS spectra were acquired with a Gatan 666 parallel EELS spectrometer attached to a Philips 400ST-FEG transmission electron microscope (TEM) operating at an accelerating voltage of 100 keV. Details of the PEELS experimental procedure and

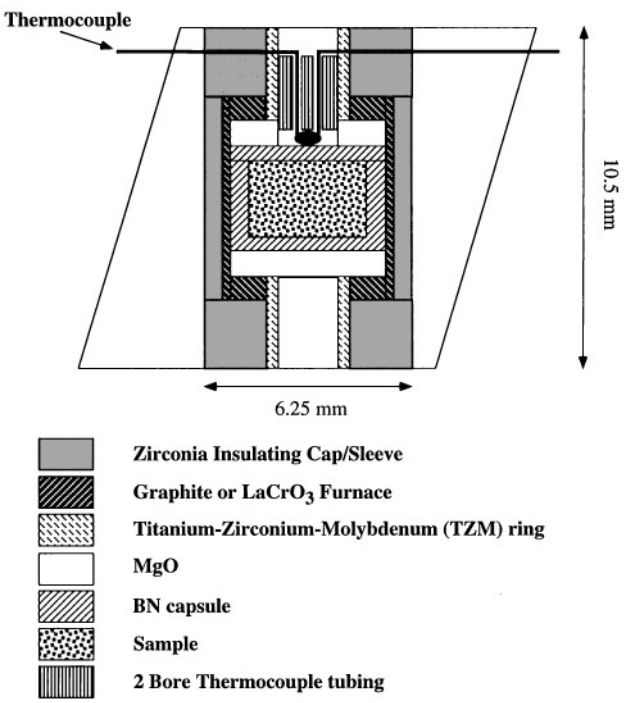

FIG. 2. Schematic of the cell assembly. The reaction mixtures are contained in the 3.2-mm diameter by 3.2-mm high hexagonal BN capsule. This 6.25×10.5 mm assembly is placed at the center of an MgO octahedron to which pressure is applied isostatically.

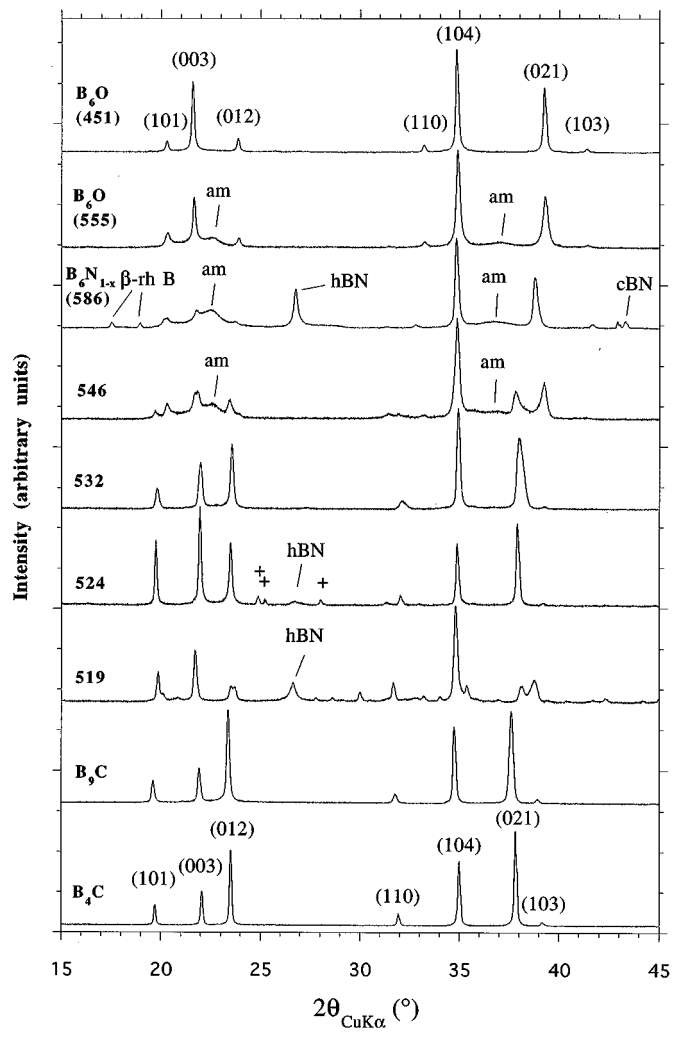

FIG. 3. Powder X-ray diffraction patterns of samples 519, 524, 532, 546, and 586 (B_6N_{1-x}) compared with B_6O (451 and 555), B_9C, and B_4C. (+ unidentified reflections; β-rh B, β-rhombohedral B; am, amorphous B; h BN, hexagonal BN; and cBN, cubic BN).

data analysis are described in (9). The morphologies and particle sizes of selected samples were studied by scanning (SEM) and transmission electron microscopy (TEM).

3. RESULTS AND DISCUSSION

(a) B–C–O System

In each run (Table 1), a partial reaction was observed at the interface between the hexagonal BN capsule and the starting materials. The run products were carefully recovered to reduce BN contamination. Only the inner parts of the samples were studied in this investigation. Details of the PEELS study is given in part II (9), in which bulk reaction products and interfacial products were examined.

In the first set of experiments (runs 519, 521, 524, and 532), prepared according to Eq. [2], XRD revealed the presence of new phases together with a small amount of amorphous material, attributed to the matrix in which the $B_xC_yO_z$ materials are formed. This amorphous material may result from excess boron oxide or boric acid and was easily removed by washing the samples in water. XRD patterns are shown for 2θ from 15° to 45° (Fig. 3) and compared to the powder pattern of B_6O and the two boron carbide end-members, B_9C and B_4C (CERAC). The patterns of the run products show reflections not observed in the pure end-members.

Sample 519 is reddish-brown (darker than B_6O synthesized by high pressure (10)). The XRD pattern (Fig. 3) shows reflections related to the pattern of B_6O and B_4C but could not be assigned to a single phase. The most intense reflection at 2.575 Å ($2\theta_{CuK\alpha} = 34.84°$) matches that for B_6O ($d_{104} = 2.571$ Å, $2\theta_{CuK\alpha} = 34.90°$) whereas reflection $d_{021} = 2.293$ Å ($2\theta_{CuK\alpha} = 39.29°$, $I/I_0 = 65$), expected for B_6O, is not observed, and no other major reflection closely matches the B_6O pattern. Moreover, the powder pattern of 519 displays additional lines in comparison to B_4C and B_6O together with splitting and peak broadening of several reflections. These observations support the hypothesis of the presence of more than one α-rhombohedral B-type $B_xC_yO_z$ phase in the sample. Quantitative analysis performed using PEELS confirmed this interpretation, and $B_xC_yO_z$ phases with B K edges typical of α-rhombohedral boron-rich solids were identified. A wide range of compositions from $B_{6.5}C$ to $B_6C_{0.45}O_{0.77}$ was observed. N contents, to 5 at.%, were detected in some of the α-rhombohedral B materials, presumably derived from the BN capsule.

Run products 521 and 532 are brownish-red crystals in a grayish-white matrix. The XRD pattern (Fig. 3) of the washed sample reveals reflections consistent with a material intermediate between "B_4C" and B_6O. It presents similarities to the pattern of boron carbides but, as for B_6O, d_{104} is the most intense XRD line. Two reflections, corresponding to reflection (110) and (021) of "B_4C" and B_6O, show broadening. The asymmetry of reflections suggests the presence of several materials of close stoichiometry. PEELS supported this result and crystals related to the

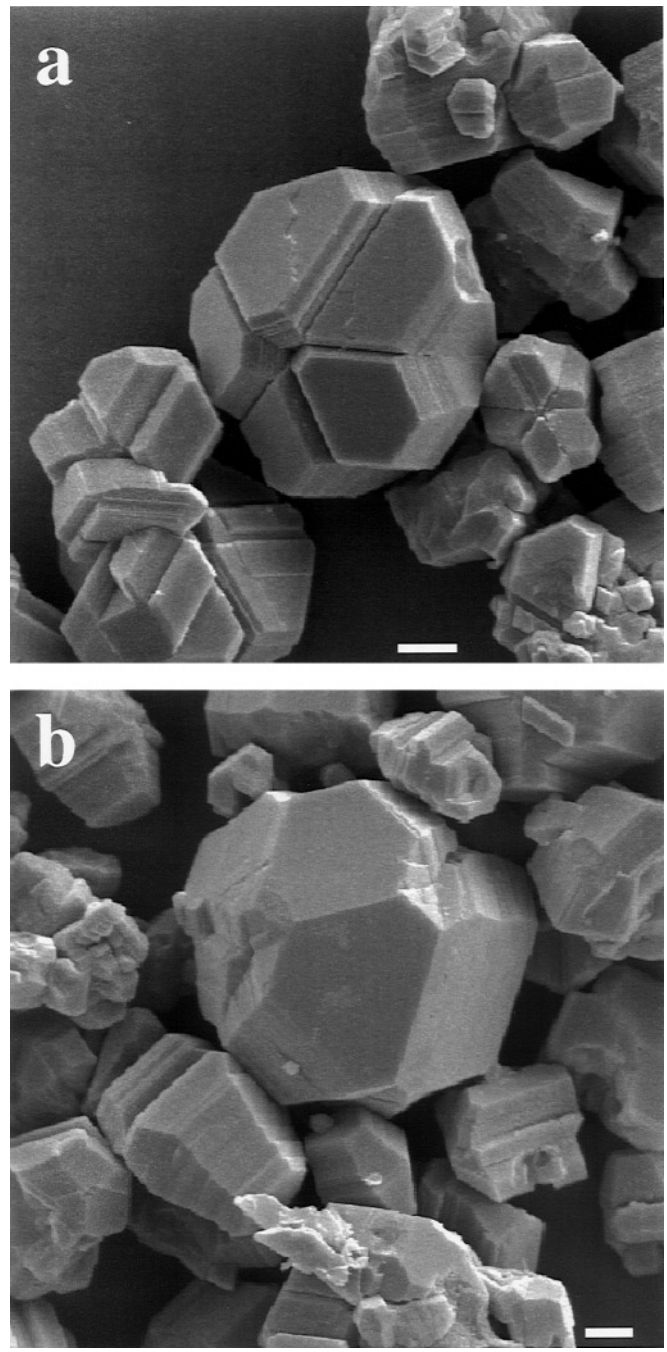

FIG. 4. SEM images of sample 524 showing a range of particle morphologies. (a) Fivefold cyclic twinned particles and (b) twinned particles with an approximate icosahedral shape. The bulk of the particles are hexagonal dipyramids with a well-developed (0001) pinacoid. Scale bars represent 2 μm.

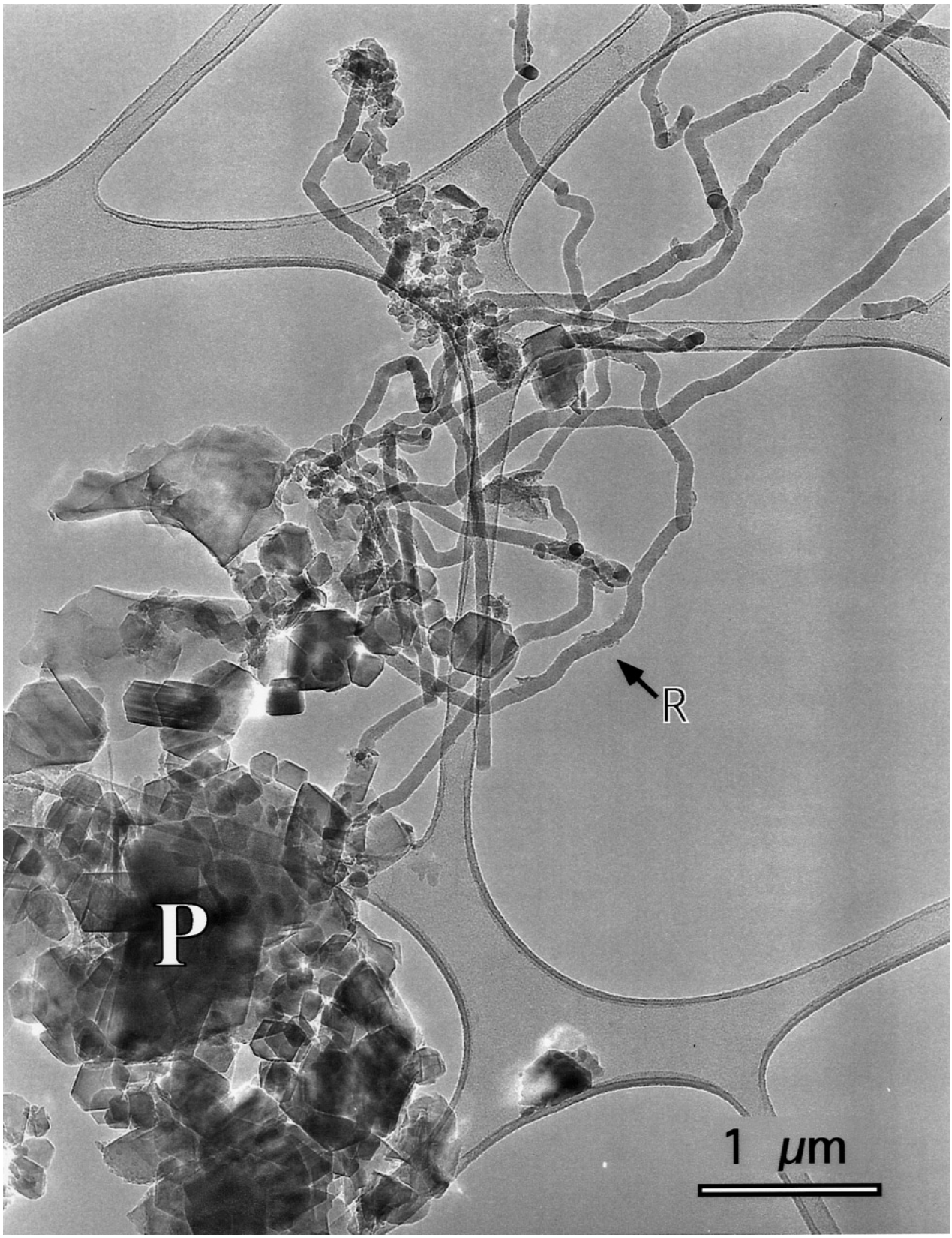

FIG. 5. TEM image of sample 532 showing "B_4C" nanorods (R) and polyhedral particles (P) of "B_4C".

TABLE 2
Hexagonal Cell Parameters for Selected Compounds Related to the α-Rhombohedral B Structure (Space Group $R\bar{3}m$)

Compound	a_h (Å)	c_h (Å)	c_h/a_h	V(Å^3)	Ref.
α-rh B	4.927(3)	12.564(7)	2.550	264.1	(10)
$B_6O_{0.96}$	5.390(1)	12.313(1)	2.284	309.8	(11)
$B_6C_{1.1}O_{0.33}$	5.570(2)	12.117(3)	2.175	325.5	This study
$B_6C_{1.28}O_{0.31}$	5.582(1)	12.135(3)	2.174	327.5	This study
B_4C	5.6039(4)	12.0786(14)	2.155	328.5	(12)
$B_{13}C_2$	5.633(1)	12.164(2)	2.159	334.3	(13)
$B_{9.3}C$	5.6720(3)	12.1428(2)	2.141	338.2	(14)
$B_{13}C_2Si_{0.03}$	5.584(1)	12.301(2)	2.223	340.9	(15)
B_4CAl_x	5.6640(3)	12.4399(12)	2.196	345.6	(1)
$B_6N_{0.92}$	5.457(7)	12.241(15)	2.243	315.7	This study
B_4N[a]	5.682(15)	12.117(58)	2.132	338.8	(16)

Note. Estimated standard deviations (ESD) are given in parentheses.
[a]We refined these cell parameters according to XRD reflections given in (16).

α-rhombohedral B type were identified with compositions near $B_6C_{1.1}O_{0.33}$ and occasionally "B_4C" containing minor O.

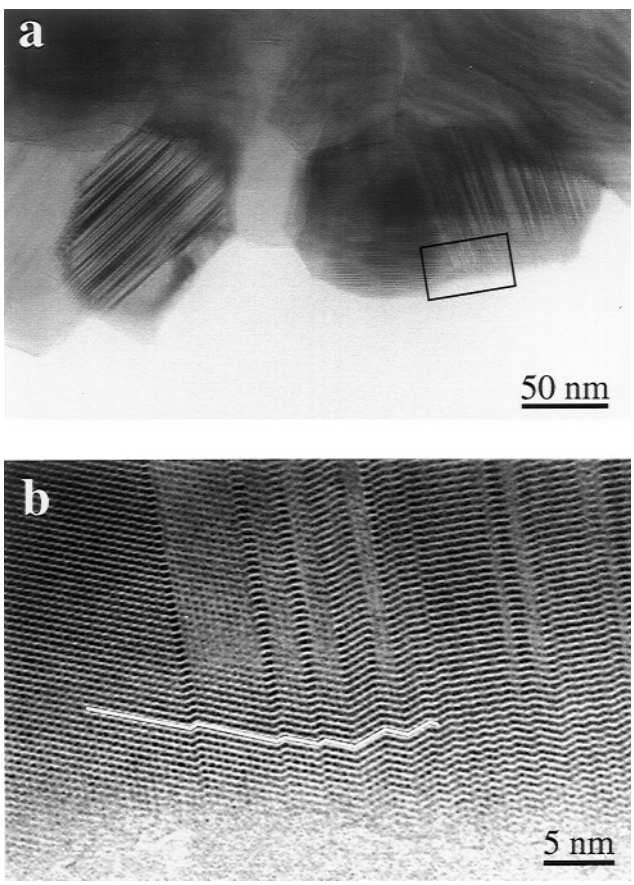

FIG. 6. TEM images of sample 550 showing (a) packing of rounded anhedral particles and (b) high-resolution image of the boxed region in (a) revealing abundant stacking faults.

Run 524 was carried out with a starting mixture identical to runs 521 and 532; it is the only run carried out with success at 5.5 GPa. Many attempts at this pressure resulted in the blow out of the assembly, a problem attributed to excess B_2O_3 (in the starting mixture) which is molten under the applied conditions. This liquid creates an unstable medium in the cell assembly, and the sample squirts out of the capsule. Higher pressures result in a better confinement of the sample and an increase in the melting point of B_2O_3. Assembly blow outs were rare at 7.5 GPa.

Crystals embedded in a soft white matrix were recovered. The crystals are copper colored in reflected light and dark brown in transmitted light. The XRD pattern for run 524 differs from runs 521 and 532. The reflections support the formation of a new phase related to the "B_4C" structure. The major position and intensity variations are observed for low-angle reflections (d_{101}, d_{003}, and d_{012}) which are significantly shifted and more intense than for B_4C. Chemical analysis of the crystals obtained by PEELS showed an average composition of $B_6C_{1.28}O_{0.31}$.

The patterns for 524 and 532 (sample assumed to be a single phase) were indexed according to the lattice symmetry of B_6O and "B_4C" and the refined hexagonal cell parameters are shown in Table 2. The cell volumes of 524 and 532 are greater than B_6O and slightly smaller than that of boron carbide phases as expected for a slight solubility of oxygen into the boron carbide framework.

SEM photographs of the α-rhombohedral boron-type $B_xC_yO_z$ crystals for sample 524 (Fig. 4) reveal euhedral crystals up to 20 μm in diameter. These crystals are in the form of hexagonal dipyramids with a (0001) pinacoid. Flattened hexagonal dipyramids forming cyclic fivefold twins (Fig. 5a) or twins that approximate the B_6O icosahedra (Fig. 4b) (11, 17) also occur.

TEM analysis of 532 revealed boron carbide nanorods (Fig. 5) together with euhedral "B_4C" crystals. These rods

vary from entangled masses to rods to 50 nm in diameter and up to a few μm in length. Most fibers were identified to be $B_6C_{0.88}$ with minor O. These rods grew in the B_2O_3 melt and small round metal inclusion occurs at their tip. The inclusions likely acts as a catalyst for their growth. PEELS of the metal inclusions show Ti, Fe, and Cr (likely from the steel die used to prepare pellets of the starting materials). The spherical beads of molten metals are considered to form during the experiment and thought to dissolve some B and C. The boron carbide precipitates from the supersaturated solution and the nucleation and growth of nanorods is observed. The boron carbide rods are comparable to those obtained by vapor–liquid–solid (VLS) mechanism (18) but we believe that the mechanism controlling the growth of our nanorods is similar to the solution–liquid–solid (SLS) process proposed by Trentler *et al.* (19).

Results of the second set of experiments (runs 545, 546, 549, and 550), carried out according to Eq. [3] are summarized in Table 1. All run products consist of hard, well-sintered aggregates. No single phase intermediate between B_6O and B_4C was identified with XRD. The samples are, reddish-black lumps with translucent red areas when observed by optical microscopy.

Sample 545, reacted with a B/C molar ratio of 4, was identified by XRD and PEELS to contain a phase close to "B_4C" with minimal O. Runs 546 and 549 have identical ratios of B to C (8 : 1); 549 was maintained at 1700°C for 5 h and 546 for 30 min. Holding the sample at that temperature for a longer time did not generate any change in XRD patterns revealing a mixture of B_6O and B_4C (Fig. 3). Peak broadening is also observed for reflections d_{021} of B_6O and "B_4C" which could be interpreted as a solution of O into the boron carbide framework and a solution of C into B_6O. Furthermore, two broad humps occur at $2\theta = 22.5^\circ$ and 37°. The same features were detected for a sample of B_6O (sample 555) prepared according to Eq. [1] at the same pressure and temperature (11). B_6O identified by PEELS together with grains of composition ranging from $B_6C_{1.28}O_{0.2}$ to $B_6C_{0.58}O_{0.46}$.

The powder pattern of run 550 (B : C = 16) shows B_6O and weak "B_4C" reflections, and no sign of solid solution is detected. The grains were identified by PEELS to be predominantly B_6O, with some grains of B_4C. Intermediate compositions, $B_6C_{0.20}O_{0.83}$, $B_6C_{0.63}O_{0.49}$, to

TABLE 3
Observed Reflections for B_6N and B_6O (Sample 451)

			B_6N		B_6O	
h	*k*	*l*	$d_{spacing}$ (Å)	Intensity (I/I_0)	$d_{spacing}$ (Å)	Intensity (I/I_0)
1	0	1	4.375[a]	17	4.371	14
0	0	3	4.075[a]	24	4.112	71
0	1	2	3.750[a]	13	3.725	17
1	1	0	2.728	10	2.695	10
1	0	4	2.572	100	2.571	100
0	2	1	2.320	59	2.293	65
1	1	3	—	—	2.253	5
0	1	5	—	—	2.180	7
2	0	2	—	—	1.860	6
2	0	5	1.705	4	1.695	4
1	0	7	1.665	5	1.648	5
1	1	6	1. 639	4	1.634	4
0	1	8	1.469	12	1.463	9
3	0	3	—	—	1.455	8
2	1	$\bar{5}$	1.435	13	1.435	10
0	2	7	1.405	3	1.405	3
2	2	0	1.365	6	1.347	7
2	0	8	1.293	6	1.286	5

[a] The position and intensity of these reflections are affected by the presence of a broad hump in this region.

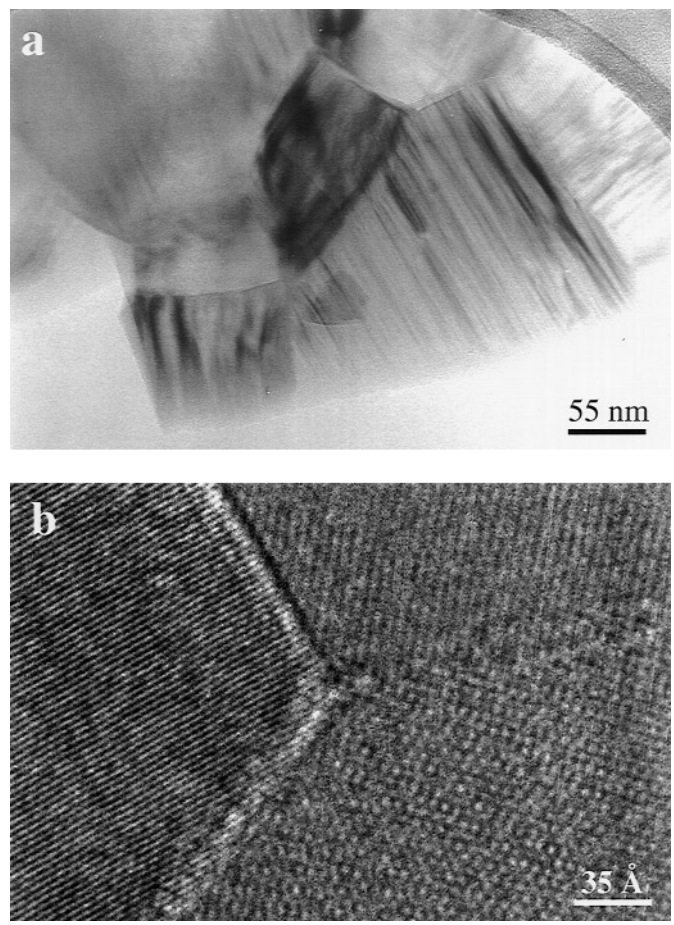

FIG. 7. TEM pictures of sample 586 showing (a) well-sintered anhedral grains and (b) the sharp junction between three B_6N crystals. The differences in lattice fringes in (b) are caused by the different orientations of the three crystals.

$B_6C_{1.2}O_{0.24}$, also occurred. TEM of the sintered materials revealed well-packed, rounded to angular, well-sorted, subhedral to anhedral grains to 1 μm (Fig. 6). These grains exhibit abundant stacking faults (Fig. 6b), similar to those in B_6O (10).

(b) B–N System

We prepared a new boron nitride compound, B_6N_{1-x}, based on the α-rhombohedral B structure according to Eq. [4] (run 586). Indications for the existence of B_6N were given by Condon *et al.* (20) and Saitoh *et al.* claimed the synthesis of B_4N using chemical vapor deposition (16) but the evidence for its existence was inconclusive. The XRD pattern (586) of a starting mixture (B/N = 6) treated at 7.5 GPa and 1700°C is given in Fig. 3. The sample is a hard grayish-black sintered mass with a metallic luster. The powder pattern of 586 shows similarities to the pattern from B_6O. Reflections from β-rhombohedral B, cubic and hexagonal BN are also observed. As with sample 555 (B_6O), an amorphous material is also detected. The *d*-spacings for B_6N_{1-x} (Table 3) resemble those of B_6O and are presumably derived from the same structure type. The refined cell parameters of our B_6N_{1-x} (Table 3) are $a_h = 5.457$ Å and $c_h = 12.241$ Å. This result is different from the finding of Saitoh *et al.* (16). We refined the cell parameters of Saitoh's B_4N, $a_h = 5.682$ Å and $c_h = 12.117$ Å ($V = 338.5$ Å^3), according to the four reflections listed in (16). Our B_6N_{1-x} has a cell volume of 315.7 Å^3 intermediate between B_6O, $V = 310.0$ Å^3, and B_4C, $V = 328.5$ Å^3. This observation is consistent with an increase in atomic radii from O to C.

PEELS analysis confirmed the presence of free boron (similar to β-rhombohedral boron), cBN, and hBN in run 586. The major phase has a composition of $B_6N_{0.92\pm0.05}$, as derived by PEELS, and a B K edge similar in shape to that from B_6O (see Garvie *et al.* (9) for more details on the PEELS). This stoichiometry is comparable to $B_6O_{0.96}$ reported by Hubert *et al.* (11). TEM of run 586 did not reveal euhedral crystals. Instead, the sample was well sintered, equigranular, with interlocking anhedral crystals up to 1 μm in diameter (Fig. 7). The similarities in the B K near-edge structures, the powder X-ray patterns, intermediate cell volumes, and composition similar to B_6O all lend support to the conclusion that our B_6N_{1-x} has a similar structure to B_6O based on the α-rhombohedral B structure type.

4. CONCLUSIONS

In this high-pressure, high-temperature investigation, we synthesized B-rich materials belonging to the B–C–N–O system. Intermediate phases, related to the α-rhombohedral boron structure, were prepared in the B–C–O system showing evidence of solid solution between B_4C and B_6O. Boron carbide crystals containing a significant amount of O, typically $B_6C_{1.1}O_{0.33}$ and $B_6C_{1.28}O_{0.31}$, were grown up to 20 μm in diameter for mixtures in which B and C were reacted with an excess B_2O_3. Nanorods with composition near B_6C with minor O were grown in a B_2O_3 melt.

The first bulk synthesis of B_6N_{1-x}, the nitride analogue to B_6O, was also conclusively performed. XRD and PEELS data substantiate that this material has structure related to that of α-rhombohedral B and chemical analysis of this compound showed an average composition of $B_6N_{0.92}$.

ACKNOWLEDGMENTS

We are grateful to Bertrand Devouard (Arizona State University) for his assistance with the SEM work and to T. Aselage (Sandia National Labs) for supplying the B_9C samples. This work was supported by NSF MRG DMR-91-21570 and NSF EAR-9418206 (L.A.J.G. and P.R.B.). The PEELS instrument used for this research was performed at the Center for High Resolution Electron Microscopy, at Arizona State University, established with support from The National Science Foundation (Grant DMR-89-13384).

REFERENCES

1. T. Lundström, *in* "Boron-Rich Solids, AIP Conference and Proceedings" (D. Emin, T. Aselage, C. L. Beckel, I. A. Howard, and C. Wood, Eds.), Vol. 231, pp. 186–192. Am. Inst. of Phys., New York, 1991.
2. D. Emin, *in* "Materials Research Society Symposia Proceedings" (D. Emin, T. L. Aselage, and C. Wood, Eds.), Vol. 97, pp. 3–15. Materials Research Society, Pittsburgh, PA, 1987.
3. T. L. Aselage, D. R. Tallant, J. H. Gieske, S. B. Van Deusen, and R. G. Tissot, *in* "The Physics and Chemistry of Carbides, Nitrides and Borides, NATO ASI Series E" (R. Freer, Ed.), Vol. 185, pp. 97–111. Kluwer Academic, Dordrecht, 1989.
4. H. F. Rizzo, W. C. Simmons, and H. O. Bielstein, *J. Electrochem. Soc.* **109,** 1079 (1962).
5. D. E. Lide (Ed.), "CRC Handbook of Chemistry and Physics (71st ed.)" CRC Press, Boca Raton, FL, 1991.
6. D. Walker, M. A. Carpenter, and C. M. Hitch, *Am. Mineral.* **75,** 1020–1028 (1990).
7. D. R. Petrak, R. Ruh, and B. F. Goosey, *in* "5th Materials Research Symposium," NBS Spec. Pub., Vol. 364, pp. 605–611. 1972.
8. H. Bolmgren, T. Lundström, and S. Okada, *in* Boron-Rich Solids, AIP Conference and Proceedings" (D. Emin, T. Aselage, C. L. Beckel, I. A. Howard, and C. Wood, Eds.), Vol. 231, pp. 197–200. Am. Inst. of Phys., New York, 1991.
9. L. A. J. Garvie, H. Hubert, W. T. Petuskey, P. F. McMillan, and P. R. Buseck, *J. Solid State Chem.* **133,** 365 (1997).
10. B. Morosin, A. W. Mullendore, D. Emin, and G. A. Slack, in "Boron-Rich Solids, AIP Conference and Proceedings" (O. Emin, T. Aselage, C. L. Beckel, I. A. Howard, and C. Wood, Eds.), Vol. 140, pp. 197–200. Am. Inst. of Phys., New York, 1986.
11. H. Hubert, B. Devouard, L. A. J. Garvie., P. R. Buseck, W. T. Petuskey, and P. F. McMillan, (submitted) for publications.
12. A. C. Larson, *in* "Boron-Rich Solids, AIP Conference Proceedings" (D. Emin, T. Aselage, C. L. Beckel, I. A. Howard, and C. Wood, Eds.), Vol. 140, pp. 109–113. Am. Inst. of Phys. New York, 1986.

13. A. Kirfel, A. Gupta, and G. Will, *Acta Crystallogr. B* **35,** 1052–59 (1979).
14. H. L. Yackel, *Acta Crystallogr. B* **31**, 1797–1806 (1975).
15. B. Morosin, T. L. Aselage, and R. S. Feigelson, *in* "Materials Research Society Symposia Proceedings" (D. Emin, T. L. Aselage, and C. Wood, Eds.), Vol. 97, pp. 145–149. Materials Research Society, Pittsburgh, PA, 1987.
16. H. Saitoh, K. Yoshida, and W. A. Yarbrough, *J. Mater. Res.* **8,** 8–11 (1993).
17. H. Hubert, B. Devouard, L. A. J. Garvie, M. O'Keeffe, P. R. Buseck, W. T. Petuskey, and P. F McMillan, In preparation.
18. I. D. R. Mackinnon, and K. L. Smith, i*n* "Materials Research Society Symposia Proceedings" (D. Emin, T. L. Aselage, and C. Wood, Eds.), Vol. 97, pp. 127–132. Materials Research Society, Pittsburgh, PA, 1987.
19. T. J. Trenler, K. M. Hickman, S. C. Goel, A. M. Viano, P. C. Gibbons, and W. E. Buhro, *Science* **270,** 1791–1794 (1995).
20. J. B. Condon, C. E. Holcombe, D. H. Johnson, and L. M. Steckel, *Inorg. Chem.* **15,** 2173–2179 (1976).